Comparative analysis of robust inter-controller performance applied to a magnetic levitator

Carlos-Chávez Guzmán [a] *, Keyla-Gómez Urtiz* [b]

[a] Universidad Autónoma de Baja California, cchavez@uabc.edu.mx, Tijuana, Baja California, México.
[b] Universidad Autónoma de Baja California, kgomez67@uabc.edu.mx, Tijuana, Baja California, México.

Abstract

This paper presents a comparative analysis of the performance of two robust control strategies applied to a magnetic levitation (Maglev) system, characterized by its nonlinear dynamics and inherent instability. A local controller based on linear $\mathcal{H}_\infty$ control techniques was designed, evaluated in a closed-loop manner, and contrasted with a previously reported global sliding mode controller under equivalent experimental conditions. The problem formulation included nonlinear modeling of the system, incorporating parametric uncertainties and external disturbances, followed by a linearization process around the equilibrium point for the synthesis of the $\mathcal{H}_\infty$ controller. Both controllers were implemented in the Magnetic Levitation Systems 33-210 training module from Feedback Ltd., and their performance was evaluated using statistical metrics such as the mean square error (MSE) and the standard deviation (SD) with respect to the operating point. The experimental results indicate that the $\mathcal{H}_\infty$ controller offers improved stability, lower sensitivity to disturbances, and reduced power consumption, while the sliding-mode controller exhibited oscillations and peak overshoots, attributable to chattering. In conclusion, the $\mathcal{H}_\infty$ controller is more efficient for this specific system, while sliding-mode control is more suitable in environments with high uncertainty.

Keywords— Local controller, Magnetic levitation system, Robustness, Sliding mode control, Stability.

Resumen

Este trabajo presenta un análisis comparativo del desempeño de dos estrategias de control robusto aplicadas a un sistema de levitación magnética (Maglev), caracterizado por su dinámica no lineal e inestabilidad inherente. Se diseñó un controlador local basado en técnicas lineales de control $\mathcal{H}_\infty$, el cual fue evaluado en lazo cerrado y contrastado con un controlador global por modos deslizantes, previamente reportado en la literatura, bajo condiciones experimentales equivalentes. La formulación del problema incluyó el modelado no lineal del sistema, incorporando incertidumbres y perturbaciones externas, seguido de un proceso de linealización alrededor del punto de equilibrio para la síntesis del controlador $\mathcal{H}_\infty$. Ambos controladores fueron implementados en el módulo didáctico Magnetic Levitation Systems 33-210 de Feedback Ltd., y su desempeño se evaluó mediante métricas estadísticas como el error cuadrático medio (MSE) y la desviación estándar (SD) respecto al punto de operación. Los resultados experimentales indican que el controlador $\mathcal{H}_\infty$ ofrece una mejor estabilidad, menor sensibilidad a perturbaciones y un consumo energético reducido, mientras que el controlador por modos deslizantes presentó oscilaciones y sobrepasos máximos, atribuibles al fenómeno de chattering. En conclusión, el controlador $\mathcal{H}_\infty$ resulta más eficiente para este sistema específico, mientras que el control por modos deslizantes es más adecuado en entornos con alta incertidumbre.

Palabras clave*: Control de modo deslizante, Controlador local, Estabilidad, Robustez, Sistema de levitación magnética.*

1. INTRODUCTION

Magnetic levitation (Maglev) systems have attracted considerable interest in various industrial applications due to their ability to eliminate mechanical contact, significantly reducing friction, wear, noise, and vibration. These systems are utilized in various applications, including high-speed trains, wind tunnels, and energy storage, among others [2–4]. In particular, attraction-based Maglev systems exhibit highly nonlinear dynamics and inherently unstable behavior. Their operating point, determined by the balance between gravitational and electromagnetic forces, requires a constant injection of energy to maintain the object's suspension [1,5]. This challenge has motivated the development of multiple control strategies aimed at stabilizing the position of the levitated object and mitigating external disturbances and model uncertainties. Among the most relevant techniques are $\mathcal{H}_\infty$ control, recognized for its asymptotic closed-loop stabilization capability and its effectiveness in mitigating both coupled and uncoupled disturbances [6–9], and adaptive control, which dynamically adjusts its parameters in response to variations in system dynamics [10,11]. The backstepping approach has also been used to ensure global stability in strict feedback systems [12]. On the other hand, sliding mode control (SMC) is widely used in the presence of parametric uncertainties and external disturbances, although its main disadvantage lies in the chattering phenomenon—high-frequency, low-amplitude oscillations in the control signal [13–17].

This contribution focuses on the comparative analysis of the closed-loop performance of two robust control strategies: a linear local $\mathcal{H}_\infty$ controller and a nonlinear global sliding mode controller, both applied to the stabilization problem of a magnetic levitation system. The evaluation is conducted through experimental implementation in the Magnetic Levitation Systems 33-210 training module from Feedback Ltd., considering coupled and external disturbances, such as sensory noise and structural uncertainty of the model.

The article is organized as follows: Section 2 presents the problem formulation; Section 3 addresses the synthesis of the $\mathcal{H}_\infty$ controller; Section 4 presents and analyzes the experimental results; and finally, Section 5 presents the conclusions and recommendations.

2. PROBLEM FORMULATION

Let the time-invariant and non-linear system of Maglev systems [2] be defined as:

$$\left.\begin{aligned}\dot{x}_1 &= x_2 \\ \dot{x}_2 &= g - \frac{L_0 x_0}{2m}\frac{i(t)^2 + w_m(t)}{x_1^2}\end{aligned}\right\} \quad (1)$$

It is proposed that all states where noise is present in the sensors be measured.

$$y = x_1 + w_y(t), \quad (2)$$

where $x_1(t) \in \mathbb{R}^1$is the distance between the sphere and the magnetic core, $x_2(t) \in \mathbb{R}^1$ is the speed with which the sphere moves, $i(t) \in \mathbb{R}^1$ is the control input, $w_m(t) \in \mathbb{R}^1$ represents the model uncertainty and external disturbances, $w_y(t) = \begin{bmatrix} w_{y1} & w_{y2} \end{bmatrix}^T \in \mathbb{R}^2$ are noise in the sensors, $g = 9.81 m/s^2$is defined as the gravitational constant, $x_0 = 0.032m$ is the operating point of the system, measured as the distance between the sphere and the magnetic core, $m = 0.02Kg$ is the mass of the sphere, and $L_0 = 89mH$ is the increase in inductance when the sphere starts moving.

Assumption 1. It is assumed that the perturbation satisfies:

$$\|w_m(t)\| \leq W^+ \quad (3)$$

where W^+ is the maximum value of the disturbance w(t), known as a priori [16].

2.1 CONTROL OBJECTIVE.

The control objective for the closed-loop system is established as follows: for some initial conditions. $\|\boldsymbol{x_1(t_0)}\| < \boldsymbol{\delta}$ and in the presence of disturbances, the following must be satisfied:

$$\lim_{t\to\infty} \|x_1(t)\| = x_0, \quad (4)$$

where $\boldsymbol{\delta = 40\,mm}$ is the diameter of the viewing cylinder installed in the phototransistor to detect the position.

Fig. 1. Magnetic levitation system.

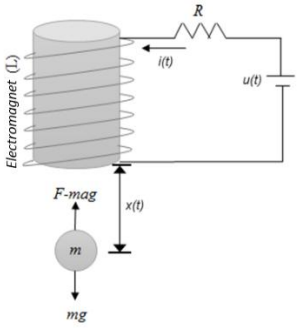

Source: [Feedback Instruments (2006)]

In the equilibrium point analysis, a homogeneous system is solved, and the dynamics of the system (1) are canceled; therefore, we obtain the following: $\boldsymbol{x_2^* = 0}$, $\boldsymbol{\beta \frac{i_0^2}{(x_1^*)^2} = g}$, where $\boldsymbol{i_0 = 0.376A}$ is the constant current needed to keep the sphere at the operating point, the state variables of the system are cleared, and according to [14] and [18], the equilibrium point of the system is shifted to the operating point $(\boldsymbol{x_1^*, x_2^*}) = (\boldsymbol{x_0, 0})$ as shown in figure 1, where $\boldsymbol{x_1^* = x_0}$, therefore, the operating region is defined as:

$$\chi = \{x(t) \in \mathbb{R}^2 : \|x(t)\| \leq \delta\}, \quad (5)$$

region where the displaced equilibrium point is located.

3. CONTROL DESIGN $\mathcal{H}_\infty$

The system (1) is linearized using Taylor series around the equilibrium point $(\boldsymbol{x_1^*, 0})$, and considering the parameters described above, the following representation is obtained in linear state spaces of the form:

$$\left.\begin{aligned}\begin{bmatrix}\dot{\bar{x}}_1 \\ \dot{\bar{x}}_2\end{bmatrix} &= \underbrace{\begin{bmatrix}0 & 1 \\ \frac{L_0 i_0^2}{m x_0^2} & 0\end{bmatrix}}_{A}\begin{bmatrix}\bar{x}_1 \\ \bar{x}_2\end{bmatrix} + \underbrace{\begin{bmatrix}0 \\ -\frac{L_0 i_0}{m x_0 R}\end{bmatrix}}_{B}\boldsymbol{u(t)} \\ \boldsymbol{y} &= \underbrace{[1 \quad 0]}_{C}\begin{bmatrix}\bar{x}_1 \\ \bar{x}_2\end{bmatrix} + \boldsymbol{w_y(t)},\end{aligned}\right\} \quad (6)$$

where $[\bar{x}_1 \quad \bar{x}_2]^T \in \mathbb{R}^2$ are the linearized states, $\boldsymbol{A} \in \mathbb{R}^{2x2}$ is the state matrix, $\boldsymbol{B} \in \mathbb{R}^2$ is the input vector, $\boldsymbol{C} \in \mathbb{R}^2$is the output vector, $\boldsymbol{u(t)} \in \mathbb{R}^2$ is the new control input, $\boldsymbol{R = 66\Omega}$ is the resistance of the electromagnet.

Table 1. Parameters of the magnetic levitator.

Parameter	Magnitude	Description
m	$0.02\ Kg$	Mass of the sphere
g	$9.81\ {}^{m}/_{s^2}$	Gravitational constant
x_0	$0.032\ m$	Distance between the sphere and the magnetic core
i_0	$0.376\ A$	Constant current
L_0	$89\ mH$	Constant Inductance
R	$66\ \Omega$	Resistance of the electromagnet
δ	$40\ mm$	The diameter of the viewing cylinder

Source: [19].

The controller design and the system (according to [6],[7],[8]) are represented in the general form $\mathcal{H}_\infty$:

$$\left.\begin{aligned}\dot{\bar{x}} &= A\bar{x} + B_1 w + B_2 u \\ z &= C_1\bar{x} + D_{12}u \\ y &= C_2\bar{x} + D_{21}w\end{aligned}\right\} \quad (7)$$

where $\boldsymbol{w(t)} = \left[\boldsymbol{w_m}\ \boldsymbol{w_y}\right]^{\boldsymbol{T}} \in \mathbb{R}^{r}$, with$\boldsymbol{w_y} = \left[\boldsymbol{w_{y1}}\ \boldsymbol{w_{y2}}\right]^{\boldsymbol{T}}$, are model uncertainty and noise in the sensors, respectively, $\boldsymbol{z(t)} \in \mathbb{R}^{l}$ is the virtual output vector control, $\boldsymbol{u(t)} \in \mathbb{R}^{m}$ is the control input, and $\boldsymbol{y(t)} \in \mathbb{R}^{p}$ is the output vector of the plant.

where $\boldsymbol{w(t)} = \left[\boldsymbol{w_m}\ \boldsymbol{w_y}\right]^{\boldsymbol{T}} \in \mathbb{R}^{r}$, with $\boldsymbol{w_y} = \left[\boldsymbol{w_{y1}}\ \boldsymbol{w_{y2}}\right]^{\boldsymbol{T}}$, are model uncertainty and noise in the sensors, respectively, $\boldsymbol{z(t)} \in \mathbb{R}^{l}$ is the virtual output vector control, $\boldsymbol{u(t)} \in \mathbb{R}^{m}$ is the control input, and $\boldsymbol{y(t)} \in \mathbb{R}^{p}$ is the output vector of the plant.

The matrices $\boldsymbol{A, B_1, B_2, C_1, D_{12}, C_2, and\ D_{21}}$ are known and have appropriate dimensions and are defined as:

$$A = \begin{bmatrix} 0 & 1 \\ 613.125 & 0 \end{bmatrix}, B_1 = \begin{bmatrix} 0 & 0 \\ 1 & 0 \end{bmatrix},\ B_2 = \begin{bmatrix} 0 \\ -52.36 \end{bmatrix},$$

$$C_1 = \begin{bmatrix} 1 & 0 \\ 0 & 1 \\ 0 & 0 \end{bmatrix}, D_{12} = \begin{bmatrix} 0 \\ 0 \\ 1 \end{bmatrix}, C_2 = [1 \quad 0],$$

$$D_{21} = [0 \quad 1].$$

According to [8],[9], the system (7) must satisfy the following assumptions:

Assumption 2. $(\boldsymbol{A, B_1})$ is controllable and $(\boldsymbol{C_1, A})$ is observable.

Assumption 3. $(\boldsymbol{A, B_2})$ is stable and $(\boldsymbol{C_2, A})$is detectable.

Assumption 4. $\boldsymbol{D_{12}}^{\boldsymbol{T}}[\boldsymbol{C_1\ D_{12}}] = [\boldsymbol{0\ I}]$.

Assumption 5. $[B_1\ D_{21}]{D_{21}}^{T} = [0\ I]^{T}$.

System (7) meets assumptions 1-5, then the control approach $\mathcal{H}_\infty$ requires a state feedback control law of the form:

$$u = \kappa(\bar{x}) \tag{8}$$

Considering the following block diagram:

Fig. 2. Block diagram of $\mathcal{H}_\infty$ control

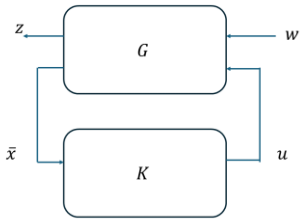

Source: [Isidori & Astolfi (1992)

Where the plant is *G,* and the control is *K*, these being real and rational.

The control objective $\mathcal{H}_\infty$ consists of designing an admissible controller such that $\|T_{ZW}\|_\infty$ exists, and with the system initialized at the equilibrium point, finding an actual number $\gamma > 0$ such that the following inequality (9) is fulfilled for a value of $w \neq 0$.

$$\int_0^t \|z\|^2 dt < \gamma^2 \int_0^t \|w\|^2\, dt \tag{9}$$

To find the solution to the $\mathcal{H}_\infty$ control problem locally for the magnetic levitation system, and the following assumptions must be met:
There is a positive definite solution to the algebraic Riccati equation:

$$KA + A^T K + {C_1}^T C_1 + K\left[\frac{1}{\gamma^2} B_1 {B_1}^T - B_2 {B_2}^T\right] K = 0, \tag{10}$$

such that the system:

$$\dot{\bar{x}} = \left[A - \left(B_2 {B_2}^T - \gamma^2 B_1 {B_1}^T\right) K\right]\bar{x}, \tag{11}$$

be exponentially stable.

If the above assumption holds, then $\kappa(\bar{x})$ is an admissible controller that solves the $\mathcal{H}_\infty$ control problem in its local form:

$$u(t) = -{B_2}^T K \bar{x}. \tag{12}$$

The Riccati algebraic equation is solved for a value of $\gamma = 0.1$, and the gain of control *K* is defined as:

$$K = \begin{bmatrix} 16.6506 & 0.4658 \\ 0.4658 & 0.0271 \end{bmatrix} \tag{13}$$

4. EXPERIMENTAL RESULTS.

The experimental validation of the control strategies was conducted using the Feedback Instruments Ltd. model 33-942S magnetic levitation training module [19], which comprises the 33-210 levitator, the 33-301 analog control interface, the 33-942 connection interface, and an Advantech PCI-1711 acquisition card. The system was operated using a Pentium-based computer with MATLAB/Simulink 2006 software. During the experiments, the state variable $\bar{x}_1$, corresponding to the position of the sphere, was measured directly by the optical sensor. The velocity $\bar{x}_2$ was estimated using the numerical derivative of $\bar{x}_1$. It should be noted that the power of the system stage incorporates an internal control that converts the input voltage signal into a proportional current, described by the relationship:

$$i(t) = 0.015u(t) + i_0, \tag{14}$$

Fig. 3. Block diagram of closed loop system

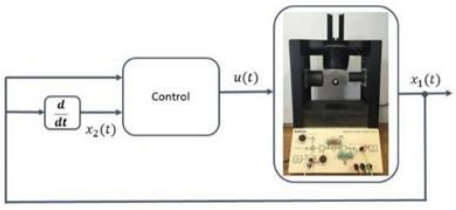

Source: [19]

where i_0 represents the current required to maintain the sphere at the operating point, and the position is also estimated from the phototransistor output voltage using:

$$\bar{x}_1(t) = \frac{v_s(t)}{120} + x_0, \quad (15)$$

where $v_s(t)$ is the voltage of the phototransistor.

We consider the coupled disturbances as uncertainty in the model (1), and the external disturbances of the system are due to the sensitivity of the phototransistor to light in the environment, which produces noise in the measurement of the state $\bar{x}_1$. The performance of the closed-loop control system is shown below, considering the position of the sphere, starting from the initial condition of $\bar{x}_1(0) = 0.046$m. The analysis of the performance of the closed-loop control system used the criterion of the Mean Square Error (MSE) and the Standard Deviation (SD) concerning the operating point; the analysis considers 10,000 samples in a time of 10 s. The performance obtained by two robust controllers, the linear $\mathcal{H}_\infty$ controller and the work reported by [1], who used a Sliding Mode Controller (SMC) applied to the same plant, are compared; Table 2 and Figures 4-7 show the summary.

The external disturbances considered include optical noise in the environment, which affects position measurement, and coupled disturbances associated with uncertainties in the model parameters. Performance evaluation was performed using two statistical metrics: the Mean Square Error (MSE) and the Standard Deviation (SD) relative to the operating point x_0. Measurements were taken over 10,000 samples within 10 seconds.

The results are summarized in Table 2 and illustrated in Figures 4-7. The $\mathcal{H}_\infty$ controller showed smooth convergence toward the equilibrium point, with a settling time of 2.5 seconds and mild underdamped oscillation (Figure 4), while its current consumption remained between 0.36 A and 0.45 A, with peaks of up to 0.6 A (Figure 5).

In contrast, the sliding-mode controller exhibited an overshoot greater than 100% (Figure 6) and a faster settling time (1.5 s) but was accompanied by oscillations associated with chattering. The control signal showed similar variations in current consumption, with peaks of 0.6 A (Figure 7).

Table 2. Root mean square error and standard deviation of the trajectory of state $\bar{x}$ *concerning* x_0.

MSE	SD	Controller
$6.0013x10^{-6}$m	0.0007 m	$\mathcal{H}_\infty$
16.037x10^{-6} m	0.0015 m	SMC

Source: [Own elaboration].

While both controllers exhibit similar performances from a practical standpoint, the $\mathcal{H}_\infty$ controller offers quantifiable advantages in terms of stability, regulation, and energy efficiency.

Fig. 4. The closed-loop trajectory of the state $\bar{x}_1$ ($\mathcal{H}_\infty$ control)

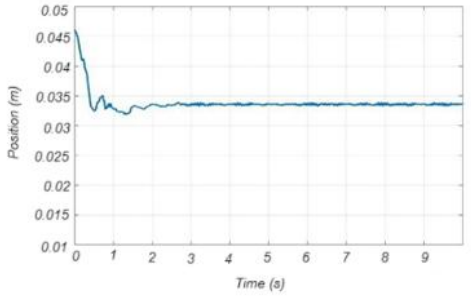

Source: [Own elaboration]

Fig. 5. Control signal *i(t)* ($\mathcal{H}_\infty$ control)

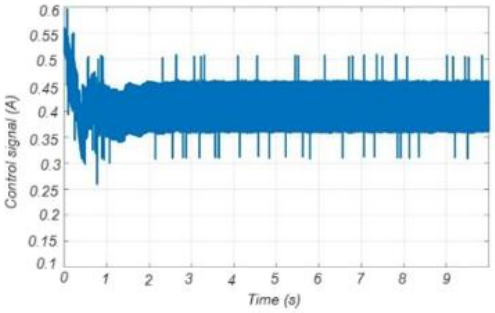

Source: [Own elaboration]

Fig. 6. The closed-loop trajectory of the state $\bar{x}_1$ (SMC)

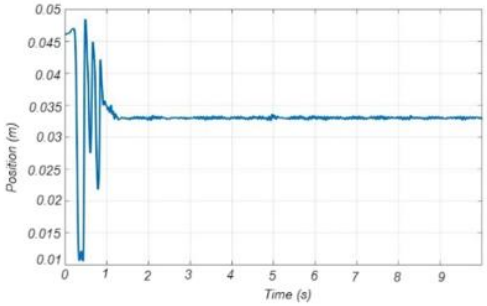

Source: [*1*]

Fig. 7. Control signal *i(t)* (SMC)

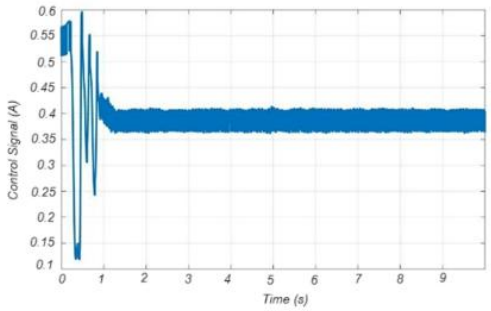

Source: [*1*]

5. CONCLUSIONS AND RECOMMENDATIONS

This study focused on the comparative evaluation of the performance of two robust control approaches applied to a magnetic levitation system within an operational region defined by the infrared sensor field of view, which contains the equilibrium point $(x_0, 0)$. Both controllers, the one based on linear $\mathcal{H}_\infty$ techniques and the nonlinear sliding mode controller, were implemented under identical experimental conditions within this region, ensuring that the comparison was conducted in a local context.

The $\mathcal{H}_\infty$ controller, designed by linearizing the system around the equilibrium point, demonstrated superior performance in terms of position control, lower sensitivity to disturbances, and reduced energy consumption, as evidenced by the statistical results presented. The sliding mode controller, while effective in the face of structural uncertainties, exhibited chattering effects, with high-frequency oscillations that affected the quality of the system's dynamic response. These findings suggest that the $\mathcal{H}_\infty$ controller is more suitable for environments where the dynamic model is well known and precise and efficient regulation is required. In contrast, sliding mode control may be preferable in scenarios where system uncertainties are significant, although the impact of chattering on the actuators and system lifetime must be considered.

It is recommended to extend this study to hybrid approaches that combine the advantages of $\mathcal{H}_\infty$ and sliding mode control, as well as to explore chatter mitigation strategies, such as second-order sliding mode control or adaptive smoothing techniques. Furthermore, it is suggested to perform real-time analyses under different disturbance profiles to evaluate the robustness of the controllers in more demanding scenarios representative of industrial applications.

6. REFERENCES

[1] Anaya Álavarez, J., and Chávez Guzmán, C. (2024). Desempeño de un control por modo deslizante aplicado al módulo didáctico del levitador magnético modelo 33-210. Aristas: Investigación Básica Y Aplicada, 10(18). ISSN 2007-9478.

[2] Khan, M. J., Junaid, M., Bilal, S., Siddiqi, S. J., and Khan, H. A. (2018). Modelling, Simulation & Control of Non-Linear Magnetic Levitation System. 2018 IEEE 21st International Multi-Topic Conference (INMIC), 978-1-5386-7536-6. https://doi.org/10.1109/inmic.2018.8595598

[3] Dušek, F., Tuček, J., Novotný, A., and Honc, D. (2023). Generalized first-principle model of magnetic levitation. Journal of Magnetism and Magnetic Materials, 587(0304-8853), 171330

[4] Xu, Z., Chanuphon Trakarnchaiyo, Stewart, C., and Mir Behrad Khamesee. (2024). Modular Maglev: Design and implementation of a modular magnetic levitation system to levitate a 2D Halbach array. Mechatronics, 99(0957-4158), 103148–103148. https://doi.org/10.1016/j.mechatronics.2024.103148.

[5] Bizuneh, A., Mitiku, H., Olalekan Salau, A., and Chandran, K. (2024). Performance Analysis of an Optimized PID-P Controller for the Position Control of a Magnetic Levitation System Using Recent Optimization Algorithms. Https://Doi.org/10.1016/J.measen.2024.101228; Elsevier Ltd.

[6] Isidori, A., and Astolfi, A. (1992). Disturbance attenuation and H_∞-control via measurement feedback in non-linear systems. IEEE Trans. Automat. Contr. 37(9), pp 1283-1293.

[7] M.D.S. Aliyu. (2017). Non-linear H-Infinity Control, Hamiltonian Systems and Hamilton-Jacobi Equations. CRC Press.

[8] Orlov, Y. V., and Aguilar, L. T. (2014). Advanced H∞ Control Towards Nonsmooth Theory and Applications. New York, Ny Springer, Imprint: Birkhäuser.

[9] John C., D., Keith, G., Pramod P., K., and Bruce A., F. (1989). State-Space Solutions to Standard H_2 and H_∞ Control Problems. IEEE Trans. Aut. Ctrl. 34 (8): pp. 831-847.

[10] Lozano, R. (2012). Adaptive Control. Springer Science & Business Media.

[11] Shao, K. (2024). Adaptive tracking control of a magnetic levitation system based on class K∞ function. European Journal of Control, 76(0947-3580), 100963–100963. https://doi.org/10.1016/j.ejcon.2024.100963.

[12] Singh, B. K., and Kumar, A. (2018). Backstepping Approach based Controller Design for Magnetic Levitation System. 2018 5th IEEE Uttar Pradesh Section International Conference on Electrical, Electronics and Computer Engineering (UPCON), 1–6. https://doi.org/10.1109/UPCON.2018.8596885.

[13] Anh Tuan Vo, Thanh Nguyen Truong, Kang, H., and Tien Dung Le. (2024). A fixed-time sliding mode control for uncertain magnetic levitation systems with prescribed performance and anti-saturation input. Engineering Applications of Artificial Intelligence, 133(0952-1976), 108373–108373. https://doi.org/10.1016/j.engappai.2024.10837.

[14] Fallaha, C., Kanaan, H., and Saad, M. (2005). Real time implementation of a sliding mode regulator for current-controlled magnetic levitation system. Mediterranean Conference on Control Automation, Lymassol, Cyprus.

[15] Fridman, L., Poznyak, A., and Francisco Javier Bejarano. (2014). Robust Output LQ Optimal Control via Integral Sliding Modes. Springer.

[16] Vadim Utkin, Guldner, J., and Shi, J. (2017). Sliding Mode Control in Electro-Mechanical Systems. CRC Press.
[17] Khalil, H. K. (2014). Non-linear Control. Prentice Hall.
[18] Freeman, R. A., and Kokotovic, P. V. (2009). Robust Non-linear Control Design. Springer Science & Business Media.
[19] Feedback Instruments. (2006). Manual Magnetic levitaction control experiments 33-942S. Feedback Instruments Ltd. www.fbk.com.